Computational and Theoretical Chemistry 1168 (2019) 112607

Contents lists available at ScienceDirect

Computational and Theoretical Chemistry

journal homepage: www.elsevier.com/locate/comptc

Oxygen reduction reaction on TiO_2 rutile (1 1 0) surface in the presence of bridging hydroxyl groups

Ádám Ganyecz[a,*], Pál D. Mezei[a,b], Mihály Kállay[a]

[a] Department of Physical Chemistry and Materials Science, Budapest University of Technology and Economics, Budapest P.O. Box 91, H-1521, Hungary
[b] Department of Chemistry, University of Basel, Klingelbergstrasse 80, CH-4056 Basel, Switzerland

ARTICLE INFO

Keywords:
Reaction mechanism
Catalysis
Oxygen reduction reaction
Rutile

ABSTRACT

The goal of this study is to provide insight into the mechanism of the oxygen reduction reaction on the TiO_2 rutile (1 1 0) surface in the presence of bridging hydroxyl groups. Considering the Langmuir–Hinshelwood and Eley–Rideal mechanisms, each possible intermediate was identified using density functional theory and a cluster model along with the energy barriers of the reduction steps and the O—O bond breaking. Our results show that the initial step, the O_2 adsorption on the surface, is favored compared to the pure surface. At higher potentials, the oxygen reduction reaction was found to go through the formation of HO_2, which can easily convert to two terminal hydroxyl groups. The rate-limiting step is the desorption of the first H_2O with 0.58 eV energy requirement at zero applied potential, while at 1.23 V the reduction of the adsorbed OH to form H_2O is the bottleneck with a barrier height of 1.71 eV.

1. Introduction

Polymer electrolyte fuel cells (PEFC) are widely investigated, because they are promising alternatives to petroleum-based energy sources due to their high efficiency, high power density, low emission, and low operating temperature [1]. However, there are still many challenges to be tackled before PEFCs can be commercialized. One of them is to find a sufficiently active and cost-effective catalyst for the oxygen reduction reaction (ORR). Nowadays Pt is used as a cathode catalyst, but the insufficient activity and high cost prevent its large-scale applications. TiO_2 is a possible candidate owing to its high stability in acidic media. It has been used in several experiments as ORR catalyst itself [2–11] and also combined with other materials [12–14]. These results show that the activity of pure TiO_2 rutile is moderate compared to Pt, but it can be increased with doping [13,14] or introducing defects on the surface [15,16]. Among the different crystal planes, the highest activity was attributed to the (1 1 0) plane [10], thus, in this work, we will focus on the TiO_2 rutile (1 1 0) surface. However, it should be mentioned that stability superior to the Pt/C catalyst and increased activity were also found introducing defects on the TiO_2 anatase (001) surface [15].

On the TiO_2 rutile (1 1 0) surface, the Ti atoms are either six- or fivefold coordinated. Furthermore, the O atoms are either threefold coordinated in the plane of the surface or twofold coordinated bridging atoms prominent from the surface. Several studies deal with the surface properties of rutile (1 1 0) [17], especially with the adsorption of H_2O and with the adsorption of small molecules on it such as water or oxygen [18–28]. The water adsorption follows an associative mechanism according to the experiments on the pure surface, while it follows a dissociative mechanism at bridging oxygen vacancies, the most common defect on this surface, leading to the formation of bridging hydroxyl groups [21,22,25].

The first step of the ORR, the oxygen adsorption on the TiO_2 rutile (1 1 0) surface, has been investigated both theoretically and experimentally in the presence of bridging hydroxyl groups. In a molecular dynamics study [29], the adsorbed OOH and hydrogen peroxide were found to be the most stable intermediates due to the stabilization by the hydrogen bonds formed with the neighboring bridging hydroxyl groups. Less stable intermediates, such as oxygen adatoms plus adsorbed water or bridging hydroxyls were not supported by the calculations. In fact, adsorbed OOH species were found to spontaneously form from the reaction of an oxygen molecule and a bridging hydroxyl group according to STM imaging [30]. The adsorbed OOH species were observed to be quite stable and immobile especially in the presence of a second bridging hydroxyl group in the vicinity, and its dissociation to an oxygen adatom and a terminal hydroxyl occurred only in few instances. As a secondary reaction, the OOH species and a neighboring bridging hydroxyl group were found to produce a water molecule

* Corresponding author.
E-mail address: ganyecz.adam@mail.bme.hu (Á. Ganyecz).

https://doi.org/10.1016/j.comptc.2019.112607
Received 22 August 2019; Received in revised form 1 October 2019; Accepted 1 October 2019
Available online 04 October 2019

leaving an oxygen adatom on the surface. The resulting oxygen adatoms turned out to be able to accept a hydrogen atom from a nearby bridging hydroxyl or from the adsorbed OOH species leading to a stable and immobile terminal hydroxyl, which can further reduce to water accepting a hydrogen atom from an adjacent bridging hydroxyl group or another terminal hydroxyl. Adsorbed hydrogen peroxide intermediate was not observed probably because of its short lifetime. On partially hydroxylated surfaces, it was also revealed that water molecules can catalyze the reaction of oxygen adatoms and bridging hydroxyls, the reaction of terminal and bridging hydroxyls, and the delivery of oxygen adatoms to bridging oxygen vacancies, which finally leads to their mutual annihilation [31]. Water molecules also resulted in shorter lifetime for the oxygen adatoms, terminal hydroxyls, and OOH species on fully hydroxylated surfaces due to the mediation of the diffusion of bridging hydroxyls to these reactants.

Despite the interest, we still lack comprehensive studies about the mechanism of the ORR on the rutile (1 1 0) surface in the presence of defects, which would facilitate the understanding of the processes and the design of better ORR catalysts. The study of defective rutile surfaces is also justified as the increased catalytic activity of the related anatase has been observed previously. In this paper, DFT methods and a cluster model are applied to examine the reduction of the oxygen molecule on the TiO_2 rutile (1 1 0) surface in the presence of bridging hydroxyl groups, taking into account the effect of the solvent and the electric potential. All the possible oxygen reduction reaction pathways are investigated, and the barriers for the O—O bond breaking and the reduction steps are determined supposing the Langmuir–Hinshelwood (LH) or the Eley–Rideal (ER) mechanisms.

2. Computational details

For the geometry optimizations and frequency calculations, the cost-efficient but still reasonably accurate BP86 semi-local generalized gradient approximation functional [32,33] was selected with the smaller 6-31G(d) basis set [34]. For the subsequent single-point energy calculations, the more accurate TPSSh functional with the larger def2-TZVP basis set [35] was utilized combined with the DFT-D3 dispersion correction [36] with Becke-Johnson (BJ) damping [37]. The density fitting approximation was invoked in all the above calculations. Open-shell systems were calculated using spin-unrestricted DFT. If it is not specified otherwise, the SMD solvation model [38] was used during the calculations. The transition states of the O—O bond breaking and the H-transfer on the surface to the reactant in the LH mechanism were confirmed by the imaginary frequency of the corresponding vibrational mode.

Free energies of the ORR intermediates were calculated based on a computational hydrogen electrode model suggested by Nørskov et al. [39], which has been used in several studies [40–44]. In this model, using the standard hydrogen electrode as reference, the chemical potential of H^+ and e^- can be related to that of $\frac{1}{2}$ H_2 in the gas phase, i.e. at $U = 0$ V, pH = 0, $p = 1$ bar, and $T = 298$ K $G(H^+) + G(e^-) = 1/2G(H_2)$. The Gibbs free energy of a species at 298 K relative to the reactants, ΔG_{298}, was calculated as

$$\Delta G_{298} = \Delta E_e(\text{solv}) + \Delta E^{\text{D3BJ}}_{\text{dispersion}} + \Delta E_{\text{ZPE}} + \Delta G_{0\rightarrow 298} + \Delta G^{\text{SMD}-\text{CDS}}_{\text{solv}} + \Delta G_U + \Delta G_{\text{pH}} \quad (1)$$

where $\Delta E_e(\text{solv})$ is the relative electronic energy calculated at the TPSSh/def2-TZVP level using SMD solvation model, while $\Delta E^{\text{D3BJ}}_{\text{dispersion}}$ is the corresponding dispersion correction. ΔE_{ZPE} and $\Delta G_{0\rightarrow 298}$ are the differences of zero-point energies and the thermal corrections to Gibbs free energies, respectively, obtained from BP86/6-31G(d) calculations. We note that the correction of Martin, Hay, and Pratt [45] was applied, i.e., in the translational partition function instead of $p = 1$ atm, $p = \rho_w RT = 1354$ atm was used to take into account the effect of the solvent on the translational entropy. $\Delta G^{\text{SMD}-\text{CDS}}_{\text{solv}}$ is the non-electrostatic effect of solvation from the SMD solvation model.

Complete frequency calculations were not feasible for our models; however, only the differences among the various species are needed to evaluate the ΔE_{ZPE} and $\Delta G_{0\rightarrow 298}$ contributions; therefore, the surface cluster model was fixed during the frequency calculations. ΔG_U incorporates the effect of the electrode potential (U), which is equal to $-eU$. ΔG_{pH} is the change in free energy due to the presence of H^+ ions in the solution, the activity of which is, however, taken as unity, so this term has no effect on the results. The energy of the reactants is $G(\text{reactants}) = G(\text{surface}) + 4[G(H^+) + G(e^-)] + G(O_2) - 4U$. For further details see the SI.

In each reduction step, which is a coupled proton and electron transfer (CPET), the proton has to surpass the double layer from the bulk solution to the electrode. The modeling of this process is out of the scope of this study, and its effect is taken into account by taking the barrier to be 0.3 eV according to Jacob et al. [46]. Therefore, the barriers of the ER mechanism are estimated to be 0.3 eV plus the reaction Gibbs free energy, if it is positive, while in the case of the barriers of the LH mechanism, the transition states of the H-transfer were also considered.

The calculations for the bigger model systems (see later) were carried out with the Turbomole 7.1 package [47]. For all the other calculations the Gaussian 09 quantum chemistry program (Revision E.01) [48] was utilized.

3. Model construction

We chose a cluster model for the description of the phenomenon studied. We note that we do not employ a periodic model, because periodic DFT calculations are still limited, compared to general DFT, regarding the available functionals (especially hybrid meta-GGA) and solvent models. Evaluation of the solvent effects are important to provide appropriate Gibbs free energy data for our processes. Also, for a periodic model a large enough cell should be used to avoid the overlap of the effect of bridging hydroxyl groups, which would be computationally demanding.

First, a pure TiO_2 rutile (1 1 0) surface model was built by cutting two trilayers from the bulk experimental rutile geometry (with Ti—O bond lengths of 1.948 Å and 1.981 Å) and closed by hydrogen atoms (with optimized positions) forming terminal hydroxyl groups, which led to a $Ti_{21}O_{54}H_{24}$ cluster (Fig. 1). Two-trilayer thickness were used to have fivefold coordinated Ti atoms on the surface. Towards the other two directions, the size of the model was chosen to have a central fivefold coordinated Ti atom on the surface with two neighboring fivefold coordinated Ti atoms, and with two neighboring bridging oxygen atoms. For the optimization of the H—O bonds in the terminal hydroxyl groups the calculations were performed with singlet spin-multiplicity in

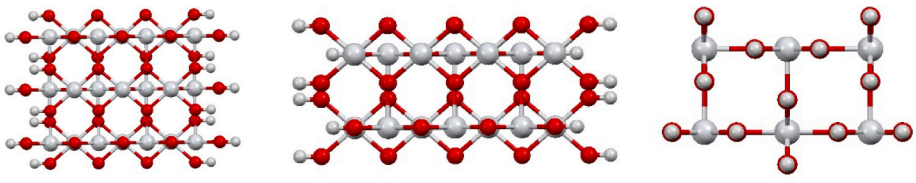

Fig. 1. The TiO_2 rutile (1 1 0) surface cluster model.

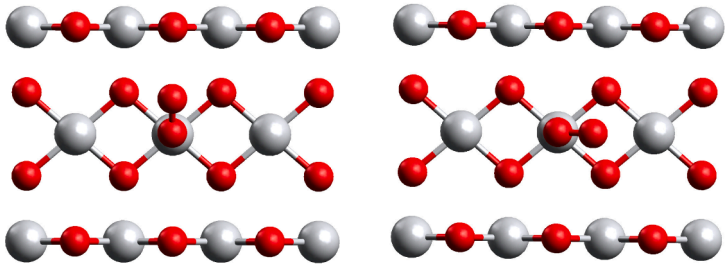

	(a) TiO_2–O_2(A)	(b) TiO_2–O_2(B)
ΔG_{ads}	0.00	0.06
$\Delta E_{ads,small}$	-0.38	-0.31
$\Delta E_{ads,big}$	-0.48	-0.40

Fig. 2. Oxygen molecule adsorbed in different orientations on the pure TiO_2 rutile (1 1 0) surface (for clarity only the upper trilayer is shown). The presented values are in eV.

gas phase.

Next, the adsorption of the oxygen molecule was investigated on the pure TiO_2 rutile (1 1 0) surface model in gas phase. Two possible stable orientations of O_2 are shown in Fig. 2. In the first one, TiO_2–O_2(A), O_2 binds perpendicularly to the line of the surface Ti atoms, while in the second orientation, TiO_2–O_2(B), O_2 is parallel. In both cases one oxygen atom binds to the Ti atom, while the other sticks out of the plane. The adsorption free energies, ΔG_{ads}, for the two orientations are fairly similar, 0.00 eV and 0.06 eV, respectively. These results are in accordance with the experimental observation: the adsorption of O_2 on pure TiO_2 rutile (1 1 0) surface is unlikely [17].

To examine the convergence of the results with respect to the cluster size, we considered the effect of the next layer (in each direction) on the oxygen adsorption energies, on a $Ti_{82}O_{194}H_{60}$ cluster. Due to the size of the system, frequency calculations were not possible, only the TPSSh-D3BJ/def2-TZVP adsorption energies were determined and compared to the results from the original model. The adsorption energies on the clusters of different size only differ by 0.10 and 0.09 eV, respectively, in the two orientations. These results support that the size of the cluster is appropriate.

To further validate our model, the gas-phase adsorption energies of H, O, OH, OOH, and H_2O were compared to literature values. The results are compiled in Table 1. Our adsorption energies only differ by 0.02, 0.03, 0.00, and 0.06 eV for H, O, OH, and OOH, respectively, from those obtained in the periodic PBE calculations of Wu [49] and Mom [50]. The conformity with the experimental data is less satisfactory: the adsorption enthalpy of H_2O is −1.57 eV from our calculations, while the experimental data is −0.96 eV [51,52]. Nevertheless, these results suggest that the applied model qualitatively correctly describes the energetics of this system, and its predictivity is similar to that of periodic DFT calculations.

In the following, a pair of bridging hydroxyl groups was built on the TiO_2 rutile (1 1 0) surface cluster model. The positions of all cluster atoms were fixed with the exception of the attached H atoms of the bridging hydroxyl groups. Using singlet and triplet spin-multiplicity for the calculation of this model with a pair of bridging hydroxyl groups it was found that the triplet state is more stable than the singlet by 0.51 eV. The resulting model system will be denoted by h-TiO_2 hereafter. Also, if necessary, the multiplicity of the system is presented in the upper left corner of the formula, for example, as ^{3}h-TiO_2.

Then, the oxygen adsorption on the surface was investigated in the presence of the bridging hydroxyl groups. Due to the hydroxyl groups the observed binding modes are different than in the case of the pure TiO_2 surface (see Fig. 3). In the first two cases, h-TiO_2–O_2(A) and h-TiO_2–O_2(B), both oxygen atoms are connected to a Ti atom, and the difference is the number of neighboring bridging hydroxyl groups. In the third possible position the two oxygen atoms attach to the same Ti atom, and the adsorbed O_2 is perpendicular to the line of the surface Ti atoms [h-TiO_2–O_2(C)]. A position similar to TiO_2–O_2(B) also exists where the O_2 molecule is stabilized by a bridging hydroxyl group [h-TiO_2–O_2(D)]. With singlet multiplicity only (A) and (B) binding modes are available with −1.34 and −1.21 eV adsorption energies, respectively. For triplet multiplicity all listed arrangements are possible, however, these are less stable than the singlet ones. The most stable triplet form is ^{3}h-TiO_2–O_2(D) with an adsorption energy of −0.92 eV, followed by ^{3}h-TiO_2–O_2(A) (−0.86 eV) and ^{3}h-TiO_2–O_2(B) (−0.85 eV), and ^{3}h-TiO_2–O_2(C) (−0.67 eV) in the stability order. These results demonstrate that the first step of the ORR, the O_2 adsorption, is energetically more favorable in the presence of bridging hydroxyl groups than on the pure surface of rutile. During the discussion of ORR mechanism, both multiplicities will be considered. Even though ^{3}h-TiO_2–O_2(D) is the most stable triplet form, ^{3}h-TiO_2–O_2(A) was used as a starting point of the ORR in the triplet case, because the possible processes (the O—O bond breaking and the first step of the reduction) are more likely from this binding mode, which is anyway by only 0.06 eV higher in energy than the most favorable orientation.

For comparison, several key features of our h-TiO_2 model agree well with the published experimental or theoretical results. The triplet state of the model is more stable than the singlet by 0.51 eV, which is quantitatively not so far from the literature value of 0.6 eV [53]. The excess electrons are localized partially on the Ti atoms between and beside the two bridging OH groups as well as partially on the fivefold coordinated surface Ti atoms near the bridging hydroxyl groups. This indicates that our model describes well the hydrated surface since the unpaired electrons tend to migrate to the surface in the presence of water according to the previous findings [54]. Moreover, in our model, the oxygen molecule is adsorbed on the surface only in the presence of bridging hydroxyl groups, which is qualitatively correct according to the literature [55].

Table 1
Adsorption energies of various species on rutile TiO_2 (1 1 0) surface compared to literature values in eV.

Species	This work	Literature	
H	−2.66	−2.64	Periodic DFT, ref [49]
O	−0.81	−0.84	Periodic DFT, ref [50]
OH	−1.56	−1.56	Periodic DFT, ref [50]
OOH	−0.62[a]	−0.56	Periodic DFT, ref [50]
H_2O[b]	−1.57	−0.96	Experimental, Refs. [51,52]

[a] The most stable binding mode has −1.18 eV adsorption energy, however, in the reference no geometry were given, we assume the same binding mode is compared here.

[b] The values are adsorption enthalpies at 298 K.

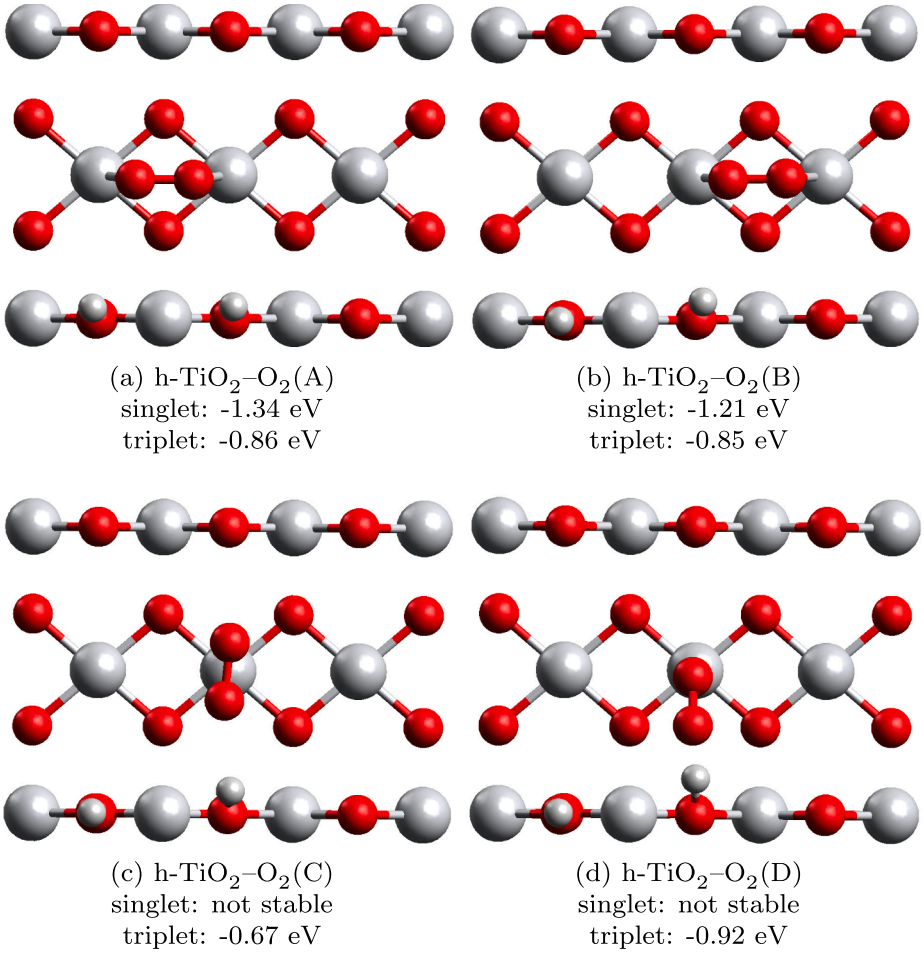

Fig. 3. Oxygen molecule adsorbed in different orientations on the TiO_2 rutile (1 1 0) surface in the presence of bridging hydroxyl groups (for clarity only the upper trilayer is shown; geometries for the triplet configurations are displayed, the geometries for the singlet configurations are similar). The adsorption energies of the oxygen molecule are shown beneath the figures.

All these findings support that our model correctly describes the energetics, electronic structure, geometry, and adhesive properties of the TiO_2 rutile (1 1 0) surface in the presence of bridging hydroxyl groups.

4. Results and discussion

Fig. 4 shows the general scheme of ORR in acidic media. In the top line the 2-electron pathway can be seen, where, after two reduction steps, H_2O_2 is formed. The requirement for the H_2O formation, i.e., the 4-electron pathway, is the cleavage of the O—O bond before the desorption of H_2O_2. Thereafter several routes are possible for the formation and desorption of H_2O.

Surface reactions can occur with the LH mechanism, where all reactants are adsorbed on the surface, or with ER, where the surface intermediate reacts with a species from the solution. In each reduction step, which is a coupled proton and electron transfer (CPET), both mechanisms were considered. Since in the LH mechanism every reduction is a two-step process, H adsorption to the surface then moving from surface to the reactants, here the higher of the two barriers is used to represent the process in these cases.

In Fig. 5 we present the free energy diagram of the ORR at 0 V potential on the TiO_2 rutile (1 1 0) surface in the presence of bridging hydroxyl groups. After the adsorption of O_2, the resulting ^{3}h-TiO_2–O_2 can be reduced to ^{2}h-TiO_2–HO_2, or the O—O bond breaking can take place to form ^{3}h-TiO_2–(O)(O). The barrier for the reduction is 0.30 eV for both the LH and the ER mechanisms, while the O—O bond breaking

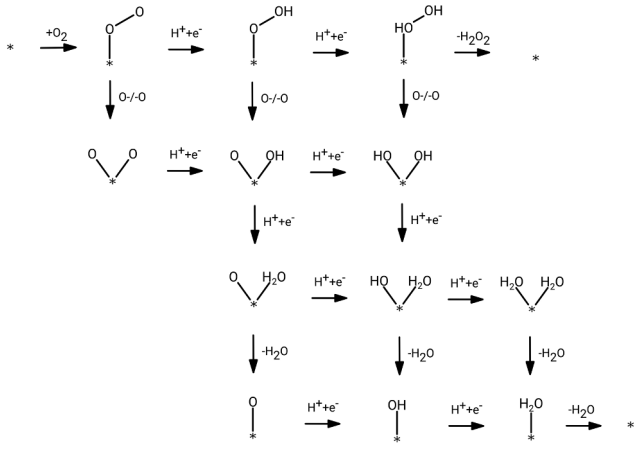

Fig. 4. Complete general scheme of the ORR mechanism on a surface in acidic media. The surface is symbolized by asterisk, O-/-O denotes bond breaking.

requires 1.11 eV. However, from the more stable ^{1}h-TiO_2–O_2 only the reduction is possible because the O—O bond breaking to form ^{3}h-TiO_2–(O)(O) is a spin-forbidden reaction, and ^{1}h-TiO_2–(O)(O) (not shown in the figure) is with 1.50 eV higher in energy than the corresponding triplet state. The barrier for the reduction is 0.31 and 0.30 eV for both the LH and the ER mechanisms, respectively, while the O—O bond breaking requires 1.11 eV, therefore the direct reduction is favored at this point.

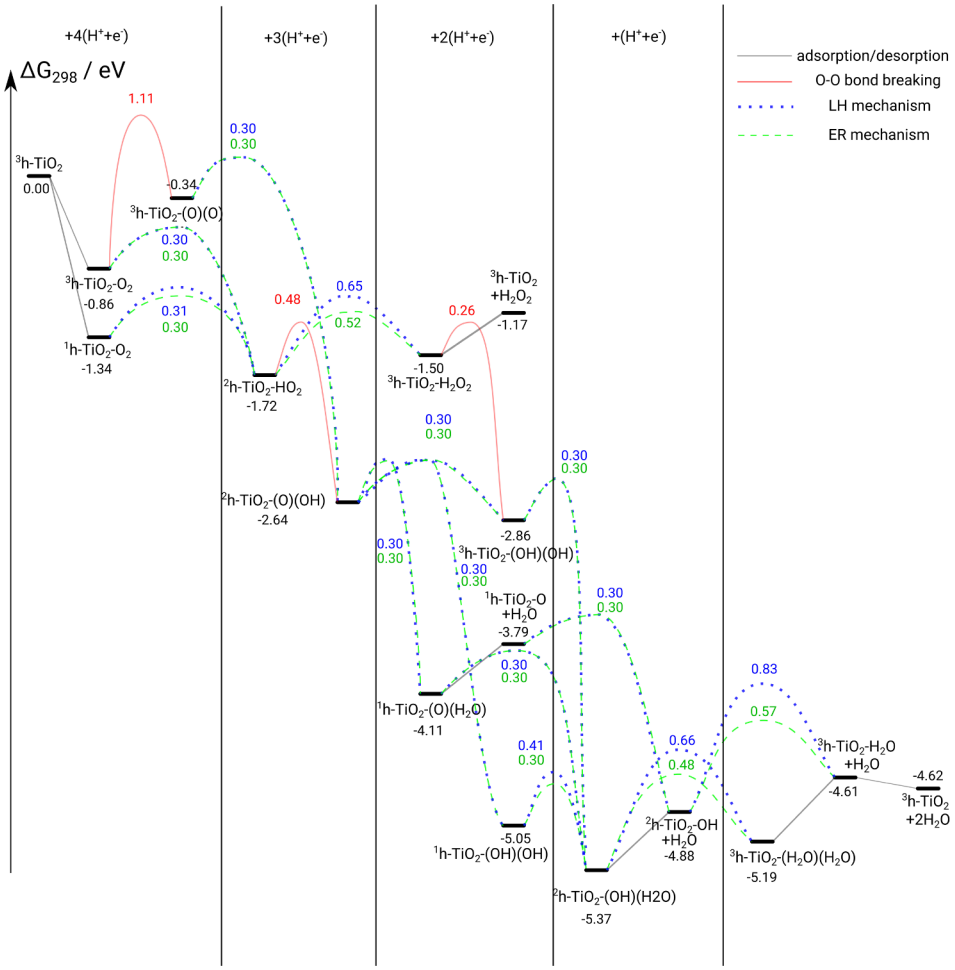

Fig. 5. Free energy diagram of ORR on TiO_2 rutile (1 1 0) surface in the presence of bridging hydroxyl groups at 0 V. Notations: grey lines: adsorption/desorption; red curves: O—O bond breaking energy barrier; blue dotted curves: energy barrier of LH mechanism; green dashed curves: energy barrier of ER mechanism. Black numbers show the free energies of the corresponding intermediates, while colored numbers are the energy barriers of the corresponding curves. All values in eV. (For interpretation of the references to colour in this figure legend, the reader is referred to the web version of this article.)

The ^{2}h-TiO_2–HO_2 can be further reduced to ^{3}h-TiO_2–H_2O_2 or can form ^{2}h-TiO_2–(O)(OH) by breaking the O—O bond. Although the latter process has the lowest barrier, 0.48 eV, reduction can also occur either through the ER or through the LH mechanism because of the low barriers of 0.52 and 0.65 eV, respectively. If the reduction pathway is followed, then the H_2O_2 formed can desorb with an energy investment of only 0.33 eV, while the formation of ^{3}h-TiO_2–(OH)(OH) from H_2O_2 requires the defeat of a 0.26 eV barrier. Thus both directions are feasible, which also means that the 2-electron pathway is possible at zero potential, however, not the main route. The formation of ^{1}h-TiO_2–(OH)(OH) from ^{3}h-TiO_2–(OH)(OH) is spin-forbidden, even though it is by 2.19 eV more stable than the triplet form.

There are again two options for the further reduction from ^{2}h-TiO_2–(O)(OH): the formation of ^{1}h-TiO_2–(O)(H_2O) or ^{1}h-TiO_2–(OH)(OH). The latter is more stable with 0.94 eV than the former, but the barriers to them are similar, 0.30 eV for both the ER and LH mechanisms.

The third reduction step produces the same intermediate, ^{2}h-TiO_2–(OH)(H_2O), from all the previous intermediates: from ^{3}h-TiO_2–(OH)(OH) and from ^{1}h-TiO_2–(O)(H_2O) with barriers of only 0.30 eV, while from ^{1}h-TiO_2–(OH)(OH) with 0.30 and 0.41 eV barrier via the ER and LH mechanisms, respectively. This is the most stable intermediate with −5.37 eV. The last reduction step to ^{3}h-TiO_2–(H_2O)(H_2O) needs 0.48 and 0.66 eV energy to overcome the barrier in the case of the ER and the LH mechanism, respectively. The desorption of the first H_2O from ^{3}h-TiO_2–(H_2O)(H_2O) requires 0.58 eV, but the desorption of the second one is spontaneous and releases 0.01 eV energy. That means that the usual coverage effect, i.e., the adsorption energy of the first molecule is the largest, the following molecules have lower adsorption energies, is not true here. The reason is that the hydrated surface is not favourable for the first H_2O adsorption, but the following H_2O molecules are stabilized by H-bridges.

The H_2O desorption can also happen earlier in the ORR, at ^{1}h-TiO_2–(O)(H_2O) or ^{2}h-TiO_2–(OH)(H_2O). In the two cases 0.32 and 0.49 eV is needed for this process, respectively. In this route, the barrier of the third reduction step from ^{1}h-TiO_2–O to ^{2}h-TiO_2–OH is 0.30 eV for both mechanisms, while, to overcome the barrier of the fourth reduction step, 0.57 and 0.83 eV is needed for the ER and LH mechanism, respectively.

If the ideal electrode potential of 1.23 V, the Nernst potential of the ORR, is applied to the system, a different energetics can be seen (see Fig. 6). The energy levels are shifted upwards with 1.23 eV after each reduction step, and the corresponding barriers are also affected. However, the O—O bond breaking barriers and the adsorption/desorption energies are unchanged.

At this potential the reduction from ^{3}h-TiO_2–O_2 to ^{2}h-TiO_2–HO_2 has a barrier of 0.67 eV in the ER mechanism, but it is still preferred over the formation of ^{3}h-TiO_2–(O)(O) with a 1.11 eV barrier. The LH barrier for this step is 1.06 eV, therefore it is not likely to occur compared to the ER mechanism. From ^{1}h-TiO_2–O_2 to ^{2}h-TiO_2–HO_2 the barriers are 1.15 and 1.54 eV for the ER and LH mechanisms, respectively. From ^{2}h-TiO_2–HO_2 the formation of ^{3}h-TiO_2–H_2O_2 is practically no longer

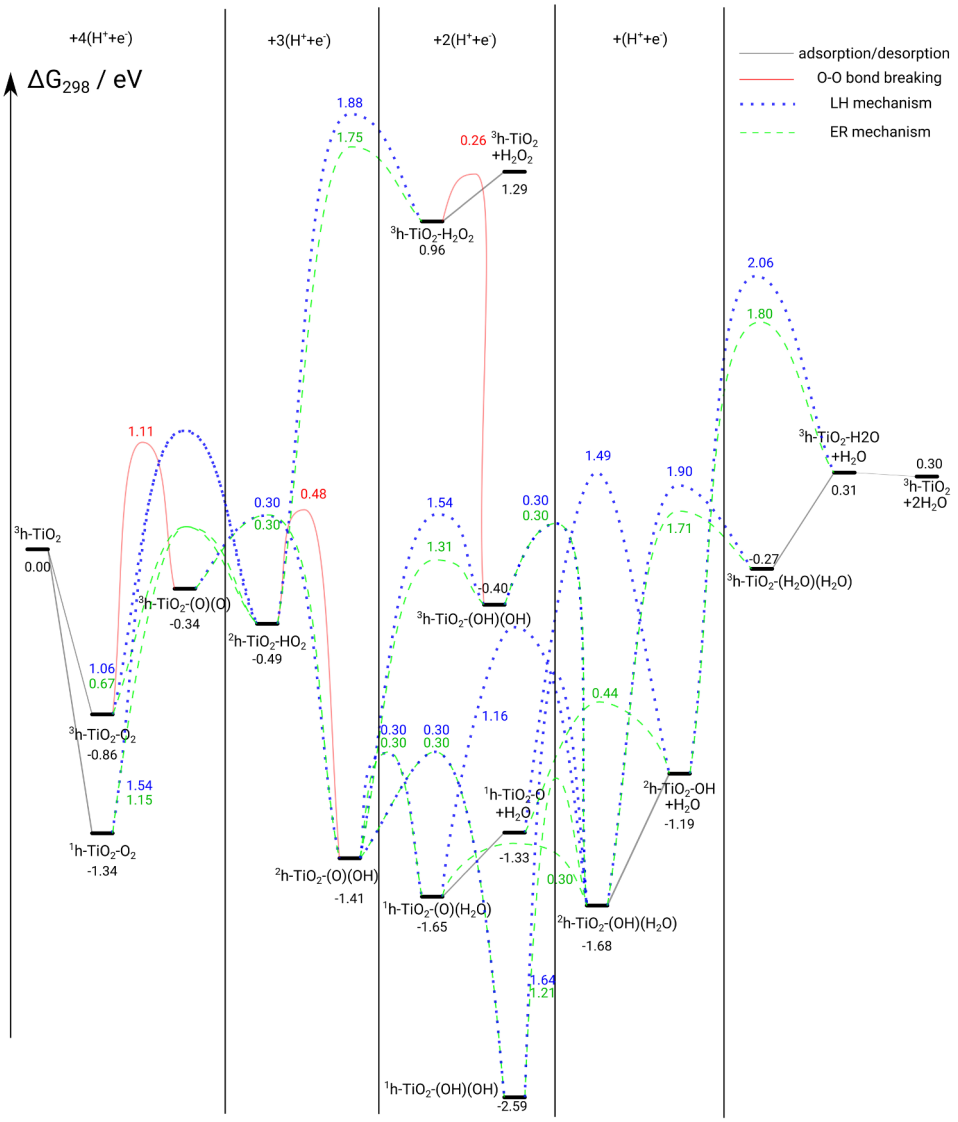

Fig. 6. Free energy diagram of ORR on TiO_2 rutile (1 1 0) surface in the presence of bridging hydroxyl groups at 1.23 V. Notations: grey lines: adsorption/desorption; red curves: O—O bond breaking energy barrier; blue dotted curves: energy barrier of LH mechanism; green dashed curves: energy barrier of ER mechanism. Black numbers show the free energies of the corresponding intermediates, while colored numbers are the energy barriers of the corresponding curves. All values in eV. (For interpretation of the references to colour in this figure legend, the reader is referred to the web version of this article.)

possible. Even the barrier with the more favorable ER mechanism is 1.75 eV, which is very high compared to the 0.48 eV barrier of the O—O bond breaking. It means that, at higher potentials, the 2-electron pathway is not possible.

The second reduction step from ^{2}h-TiO_2–(O)(OH) has a barrier of 0.30 eV to both ^{1}h-TiO_2–(O)(H_2O) and ^{1}h-TiO_2–(OH)(OH) with either mechanisms. Consequently, the lower-energy ^{1}h-TiO_2–(OH)(OH) is the preferred intermediate for this step. From both species the same intermediate, ^{2}h-TiO_2–(OH)(H_2O) is formed through the third reduction step with barriers of 1.21 and 1.64 eV for ^{1}h-TiO_2–(OH)(OH) and 0.30 and 1.16 eV for ^{1}h-TiO_2–(O)(H_2O) with the LH and ER mechanisms, respectively. However, the last reduction step requires 1.71 or 1.90 eV via the ER or the LH mechanism, respectively. The alternative pathway after the formation and desorption of the first H_2O is ^{1}h-TiO_2–O → ^{2}h-TiO_2–OH → ^{3}h-TiO_2–H_2O → ^{3}h-TiO_2. The corresponding barriers are also rather high, 0.44 and 1.80 eV for the ER, and 1.49 and 2.06 eV for the LH mechanism, respectively.

To summarize, the lowest-energy pathway at both potentials is ^{3}h-TiO_2 → ^{1}h-TiO_2–O_2 → ^{2}h-TiO_2–HO_2 → ^{2}h-TiO_2–(O)(OH) → ^{1}h-TiO_2–(OH)(OH) → ^{2}h-TiO_2–(OH)(H_2O) → ^{3}h-TiO_2–(H_2O)(H_2O) → ^{3}h-TiO_2–H_2O → ^{3}h-TiO_2, and the highest barrier to overcome at 0 V is the desorption of the first H_2O molecule with 0.58 eV, while at 1.23 V the fourth reduction step with the ER mechanism is the rate-determining step with a barrier height of 1.71 eV. It is also worth noting that, where the proton transfer through the double layer is the dominating obstacle, both the ER and the LH mechanisms can occur, but in any other case the ER mechanism is preferred.

It is also instructive to compare the mechanism of the ORR on rutile and platinum. The results of Keith and Jacob [56], who studied this process on Pt(1 1 1) surface, show that, at low potentials on Pt, the H_2O_2 formation is the preferred pathway, and a mixed 2- and 4-electron mechanism can be observed. In contrast, in our case the HO_2 pathway is favorable, and just a small amount of H_2O_2 can be expected. For Pt the rate determining step is the desorption of H_2O requiring an energy of around 0.3 eV. At 1.23 V on Pt the O—O bond breaking happens after the adsorption of O_2. The highest barrier is 0.99 eV for the last reduction step, which is almost half of the corresponding barrier for h-TiO_2. However, the rate of the first three reduction steps is expected to be similar on Pt and on the modified rutile surface even at high potentials.

All in all, our results suggest that the key steps of the 4-electron

ORR, the O_2 adsorption and the O—O bond breaking can occur on the rutile surface in the presence of bridging hydroxyl groups, which makes this material a possible ORR catalyst. However, it needs to be combined with other substances to reduce the barrier of the last reduction step of the ORR.

5. Conclusions

The reduction of the oxygen molecule was investigated on TiO_2 rutile (1 1 0) surface in the presence of bridging hydroxyl groups relying on a cluster model, which was validated using experimental and theoretical adsorption energies of H, O, OH, OOH, and H_2O. First, a pair of bridging hydroxyl groups was built on the surface locally optimizing the geometry of the cluster model. Then, using this model, the reduction reaction pathway of the oxygen molecule was investigated on the TiO_2 rutile (1 1 0) surface in the presence of bridging hydroxyl groups. The effect of solvation and potential were considered, and both the LH and the ER mechanisms were studied.

At both 0 V and 1.23 V the ORR goes through the formation of HO_2 and its dissociation and termination on the surface. Additionally, at 0 V a small amount of H_2O_2 can be expected due to the comparable barrier of the O—O bond breaking and the second reduction step. Generally, in each possible reduction step the ER mechanism is the preferred, except where the proton transfer through the double layer is the biggest obstacle. The rate-limiting step is the desorption of the first H_2O with 0.58 eV energy requirement at zero applied potential, while at 1.23 V the reduction of the adsorbed OH to form H_2O is the bottleneck with a barrier height of 1.71 eV. However, the key steps of the reaction, the O_2 adsorption and the O—O bond breaking, are possible on the surface of rutile, which makes the latter a possible mixing material for ORR catalysts.

Our findings can contribute to the understanding of the oxygen reduction reaction in polymer electrolyte fuel cells using TiO_2 rutile catalyst and to the design of more efficient electrode materials.

6. Declaration of Competing Interest

The authors declared that there is no conflict of interest.

Acknowledgement

The research within project No. VEKOP-2.3.2-16-2017-00013 was supported by the European Union and the State of Hungary, co-financed by the European Regional Development Fund and the BME-Nanotechnology FIKP grant of EMMI (BME FIKP-NAT). The computing time granted on the Hungarian HPC Infrastructure at NIIF Institute, Hungary, is gratefully acknowledged.

Appendix A. Supplementary material

Supplementary data associated with this article can be found, in the online version, at https://doi.org/10.1016/j.comptc.2019.112607.

References

[1] A. Rabis, P. Rodriguez, T.J. Schmidt, Electrocatalysis for polymer electrolyte fuel cells: recent achievements and future challenges, ACS Catal. 2 (2012) 864–890.
[2] P. Clechet, C. Martelet, J. Martin, R. Olier, Photoelectrochemical behaviour of TiO_2 and formation of hydrogen peroxide, Electrochim. Acta 24 (1979) 457–461.
[3] B. Parkinson, F. Decker, J. Juliao, M. Abramovich, H.C. Chagas, The reduction of molecular oxygen at single crystal rutile electrodes, Electrochim. Acta 25 (1980) 521–525.
[4] V.B. Baez, J.E. Graves, D. Pletcher, The reduction of oxygen on titanium oxide electrodes, J. Electroanal. Chem. 340 (1992) 273–286.
[5] Y.-K. Choi, S.-S. Seo, K.-H. Chjo, Q.-W. Choi, S.-M. Park, Thin titanium dioxide film electrodes prepared by thermal oxidation, J. Electrochem. Soc. 139 (1992) 1803–1807.
[6] T. Clark, D.C. Johnson, Activation of titanium electrodes for voltammetric detection of oxygen and hydrogen peroxide in alkaline media, Electroanalysis 9 (1997) 273–278.
[7] S. Poznyak, A. Kokorin, A. Kulak, Effect of electron and hole acceptors on the photoelectrochemical behaviour of nanocrystalline microporous TiO_2 electrodes, J. Electroanal. Chem. 442 (1998) 99–105.
[8] A. Tsujiko, H. Itoh, T. Kisumi, A. Shiga, K. Murakoshi, Y. Nakato, Observation of cathodic photocurrents at nanocrystalline TiO_2 film electrodes, caused by enhanced oxygen reduction in alkaline solutions, J. Phys. Chem. B 106 (2002) 5878–5885.
[9] S.V. Mentus, Oxygen reduction on anodically formed titanium dioxide, Electrochim. Acta 50 (2004) 27–32.
[10] J.-H. Kim, A. Ishihara, S. Mitsushima, N. Kamiya, K.-I. Ota, Catalytic activity of titanium oxide for oxygen reduction reaction as a non-platinum catalyst for PEFC, Electrochim. Acta 52 (2007) 2492–2497.
[11] Y. Liu, A. Ishihara, S. Mitsushima, N. Kamiya, K.-I. Ota, Transition metal oxides as DMFC cathodes without platinum, J. Electrochem. Soc. 154 (2007) B664–B669.
[12] K. Tammeveski, T. Tenno, A. Rosental, P. Talonen, L.-S. Johansson, L. Niinistö, The reduction of oxygen on Pt-TiO_2 coated Ti electrodes in alkaline solution, J. Electrochem. Soc. 146 (1999) 669–676.
[13] J. Li, H. Zhou, H. Zhuo, Z. Wei, G. Zhuang, X. Zhong, S. Deng, X. Li, J. Wang, Oxygen vacancies on TiO_2 promoted the activity and stability of supported Pd nanoparticles for the oxygen reduction reaction, J. Mater. Chem. A 6 (2018) 2264–2272.
[14] M. Chisaka, Y. Yamamoto, N. Itagaki, Y. Hattori, Active site formation for oxygen reduction reaction on carbon-support-free titanium oxynitride with boosted activity in acidic media, ACS Appl. Energy Mater. 1 (2018) 211–219.
[15] D.-N. Pei, L. Gong, A.-Y. Zhang, X. Zhang, J.-J. Chen, Y. Mu, H.-Q. Yu, Defective titanium dioxide single crystals exposed by high-energy {001} facets for efficient oxygen reduction, Nat. Commun. 6 (2015) 8696.
[16] G. Wang, Y. Yang, D. Han, Y. Li, Oxygen defective metal oxides for energy conversion and storage, Nano Today 13 (2017) 23–39.
[17] U. Diebold, The surface science of titanium dioxide, Surf. Sci. Rep. 48 (2003) 53–229.
[18] M. Egashira, S. Kawasumi, S. Kagawa, T. Seiyama, Temperature programmed desorption study of water adsorbed on metal oxides. I. Anatase and rutile, Bull. Chem. Soc. Jpn. 51 (1978) 3144–3149.
[19] M.B. Hugenschmidt, L. Gamble, C.T. Campbell, The interaction of H_2O with a TiO_2 (110) surface, Surf. Sci. 302 (1994) 329–340.
[20] M.A. Henderson, An HREELS and TPD study of water on TiO_2 (110): The extent of molecular versus dissociative adsorption, Surf. Sci. 355 (1996) 151–166.
[21] R. Schaub, P. Thostrup, N. Lopez, E. Lægsgaard, I. Stensgaard, J.K. Nørskov, F. Besenbacher, Oxygen vacancies as active sites for water dissociation on rutile TiO_2 (110), Phys. Rev. Lett. 87 (2001) 266104.
[22] I. Brookes, C. Muryn, G. Thornton, Imaging water dissociation on TiO_2 (110), Phys. Rev. Lett. 87 (2001) 266103.
[23] A. Bandura, D. Sykes, V. Shapovalov, T. Troung, J. Kubicki, R. Evarestov, Adsorption of water on the TiO_2 (rutile)(110) surface: a comparison of periodic and embedded cluster calculations, J. Phys. Chem. B 108 (2004) 7844–7853.
[24] S. Wendt, R. Schaub, J. Matthiesen, E.K. Vestergaard, E. Wahlström, M.D. Rasmussen, P. Thostrup, L.M. Molina, E. Lægsgaard, I. Stensgaard, Oxygen vacancies on TiO_2 (110) and their interaction with H_2O and O_2: A combined high-resolution STM and DFT study, Surf. Sci. 598 (2005) 226–245.
[25] Z. Zhang, O. Bondarchuk, B.D. Kay, J. White, Z. Dohnalek, Imaging water dissociation on TiO_2 (110): evidence for inequivalent geminate OH groups, J. Phys. Chem. B 110 (2006) 21840–21845.
[26] P.M. Kowalski, B. Meyer, D. Marx, Composition, structure, and stability of the rutile TiO_2 (110) surface: oxygen depletion, hydroxylation, hydrogen migration, and water adsorption, Phys. Rev. B 79 (2009) 115410.
[27] C. Sun, L.-M. Liu, A. Selloni, G.Q.M. Lu, S.C. Smith, Titania-water interactions: a review of theoretical studies, J. Mater. Chem. 20 (2010) 10319–10334.
[28] R. Erdogan, M.F. Fellah, I. Onal, An ONIOM and DFT study of water adsorption on rutile TiO_2 (110) cluster, Int. J. Quantum Chem. 111 (2011) 174–181.
[29] A. Tilocca, C. Di Valentin, A. Selloni, O_2 interaction and reactivity on a model hydroxylated rutile (110) surface, J. Phys. Chem. B 109 (2005) 20963–20967.
[30] Y. Du, N.A. Deskins, Z. Zhang, Z. Dohnálek, M. Dupuis, I. Lyubinetsky, Imaging consecutive steps of O_2 reaction with hydroxylated TiO_2 (110): identification of HO_2 and terminal OH intermediates, J. Phys. Chem. C 113 (2008) 666–671.
[31] Z. Zhang, Y. Du, N.G. Petrik, G.A. Kimmel, I. Lyubinetsky, Z. Dohnálek, Water as a catalyst: imaging reactions of O_2 with partially and fully hydroxylated TiO_2 (110) surfaces, J. Phys. Chem. C 113 (2009) 1908–1916.
[32] A.D. Becke, Density-functional exchange-energy approximation with correct asymptotic-behavior, Phys. Rev. A 38 (1988) 3098.
[33] J.P. Perdew, Density-functional approximation for the correlation energy of the inhomogeneous electron gas, Phys. Rev. B 33 (1986) 8822.
[34] R. Ditchfield, W.J. Hehre, J.A. Pople, Self-consistent molecular-orbital methods. IX. An extended gaussian-type basis for molecular-orbital studies of organic molecules, J. Chem. Phys. 54 (1971) 724–728.
[35] F. Weigend, R. Ahlrichs, Balanced basis sets of split valence, triple zeta valence and quadruple zeta valence quality for H to Rn: design and assessment of accuracy, Phys. Chem. Chem. Phys. 7 (2005) 3297–3305.
[36] S. Grimme, J. Antony, S. Ehrlich, H. Krieg, A consistent and accurate ab initio parametrization of density functional dispersion correction (DFT-D) for the 94 elements H-Pu, J. Chem. Phys. 132 (2010) 154104.
[37] S. Grimme, S. Ehrlich, L. Goerigk, Effect of the damping function in dispersion corrected density functional theory, J. Comput. Chem. 32 (2011) 1456–1465.
[38] A.V. Marenich, C.J. Cramer, D.G. Truhlar, Universal solvation model based on solute electron density and on a continuum model of the solvent defined by the bulk dielectric constant and atomic surface tensions, J. Phys. Chem. B 113 (2009)

6378–6396.
[39] J.K. Nørskov, J. Rossmeisl, A. Logadottir, L. Lindqvist, J.R. Kitchin, T. Bligaard, H. Jonsson, Origin of the overpotential for oxygen reduction at a fuel-cell cathode, J. Phys. Chem. B 108 (2004) 17886–17892.
[40] P. Zhang, B. Xiao, X. Hou, Y. Zhu, Q. Jiang, Layered SiC sheets: a potential catalyst for oxygen reduction reaction, Sci. Rep. 4 (2014) 3821.
[41] K. Yan, T.A. Maark, A. Khorshidi, V.A. Sethuraman, A.A. Peterson, P.R. Guduru, The influence of elastic strain on catalytic activity in the hydrogen evolution reaction, Angew. Chem. 55 (2016) 6175–6181.
[42] A.A. Peterson, F. Abild-Pedersen, F. Studt, J. Rossmeisl, J.K. Nørskov, How copper catalyzes the electroreduction of carbon dioxide into hydrocarbon fuels, Energy Environ. Sci. 3 (2010) 1311–1315.
[43] Z. Lu, G. Chen, S. Siahrostami, Z. Chen, K. Liu, J. Xie, L. Liao, T. Wu, D. Lin, Y. Liu, et al., High-efficiency oxygen reduction to hydrogen peroxide catalysed by oxidized carbon materials, Nat. Catal. 1 (2018) 156–162.
[44] Z. Wang, Z. Yu, J. Zhao, Computational screening of a single transition metal atom supported on the C_2N monolayer for electrochemical ammonia synthesis, Phys. Chem. Chem. Phys. 20 (2018) 12835–12844.
[45] R.L. Martin, P.J. Hay, L.R. Pratt, Hydrolysis of ferric ion in water and conformational equilibrium, J. Phys. Chem. A 102 (1998) 3565–3573.
[46] J.A. Keith, G. Jerkiewicz, T. Jacob, Theoretical investigations of the oxygen reduction reaction on Pt (111), ChemPhysChem 11 (2010) 2779–2794.
[47] TURBOMOLE V7.1 2016, a development of University of Karlsruhe and Forschungszentrum Karlsruhe GmbH, 1989–2007, TURBOMOLE GmbH, since 2007; available from http://www.turbomole.com.
[48] Gaussian 09, Revision C.01, M.J. Frisch, G.W. Trucks, H.B. Schlegel, et al., Gaussian, Inc., Wallingford CT, 2010.
[49] Z. Wu, W. Zhang, F. Xiong, Q. Yuan, Y. Jin, J. Yang, W. Huang, Active hydrogen species on TiO_2 for photocatalytic H2 production, Phys. Chem. Chem. Phys. 16 (2014) 7051–7057.
[50] R.V. Mom, J. Cheng, M.T. Koper, M. Sprik, Modeling the oxygen evolution reaction on metal oxides: the infuence of unrestricted DFT calculations, J. Phys. Chem. C 118 (2014) 4095–4102.
[51] C.T. Campbell, J.R. Sellers, Enthalpies and entropies of adsorption on well-defined oxide surfaces: experimental measurements, Chem. Rev. 113 (2013) 4106–4135.
[52] Z. Dohnálek, J. Kim, O. Bondarchuk, J.M. White, B.D. Kay, Physisorption of N_2, O_2, and CO on fully oxidized TiO_2 (110), J. Phys. Chem. B 110 (2006) 6229–6235.
[53] C. Di Valentin, G. Pacchioni, A. Selloni, Electronic structure of defect states in hydroxylated and reduced rutile TiO_2 (110) surfaces, Phys. Rev. Lett. 97 (2006) 166803.
[54] R. Wang, H. Fan, The location of excess electrons on H_2O/TiO_2 (110) surface and its role in the surface reactions, Mol. Phys. 116 (2018) 171–178.
[55] M. Rasmussen, L. Molina, B. Hammer, Adsorption, diffusion, and dissociation of molecular oxygen at defected TiO_2 (110): a density functional theory study, J. Chem. Phys. 120 (2004) 988–997.
[56] J.A. Keith, T. Jacob, Theoretical studies of potential-dependent and competing mechanisms of the electrocatalytic oxygen reduction reaction on Pt (111), Angew. Chem. Int. Ed. 49 (2010) 9521–9525.